



Published in final edited form as:

ACS Nano. 2012 September 25; 6(9): 7935–7941. doi:10.1021/nn302388e.

## Building a Nanostructure with Reversible Motions Using Photonic Energy

Mingxu You<sup>†</sup>, Fujian Huang<sup>†</sup>, Zhuo Chen<sup>‡</sup>, Ruo-Wen Wang<sup>†</sup>, and Weihong Tan<sup>†,‡</sup>

<sup>†</sup> Department of Chemistry, Department of Physiology and Functional Genomics, Center for Research at the Bio/Nano Interface, Shands Cancer Center, University of Florida, Gainesville, FL 32611-7200, USA

<sup>‡</sup> Molecular Science and Biomedicine Laboratory, State Key Laboratory of Chemo/Bio-Sensing and Chemometrics, College of Biology and College of Chemistry and Chemical Engineering, Hunan University, Changsha, 410082, China

### Abstract

Recently, the specific hybridization of DNA molecules has been used to construct self-assembled devices, *e.g.*, the mechanical device to mimic cellular protein motors in nature. Here, we present a new light-powered DNA mechanical device based on the photoisomerization of azobenzene moieties and toehold-mediated strand displacement. This autonomous and controllable device is capable of moving towards either end of the track, simply by switching the wavelength of light irradiation, either UV (365nm) or visible (>450nm). This light-controlled strategy can easily solve one main technical challenge for step-wise walking devices: the selection of routes in multipath systems. The principle employed in this study, photoisomerization-induced toehold length switching, could be further useful in the design of other mechanical devices, with the ultimate goal of rivaling molecular motors for cargo transport and macroscopic movement.

### Keywords

DNA nanostructure; light control; reversible motion; strand displacement

Nature has evolved various tiny protein machines (*e.g.*, myosin, kinesin and dynein) that travel along a network of tracks within the cell to transport organelles and power cellular motion.<sup>1,2</sup> Inspired by these protein-based molecular motors, artificial devices,<sup>3-7</sup> especially DNA-based motors, have recently emerged and started to mimic the function of biological motors in cargo transport<sup>6</sup> and biosynthesis.<sup>7</sup> As biological macromolecules similar in size to molecular motors, and with the added capability of simple programmable assembly, DNAs are suitable for the control of progressive, processive and directional movement at the molecular level.

Energy supply is a major concern for any motor, and various energy sources (*e.g.*, DNA hybridization,<sup>8-11</sup> hydrolysis of either DNA/RNA backbones<sup>12-15</sup> or ATP molecules<sup>16</sup>) have been previously explored for DNA walkers. Still, these artificial walkers are in their infancy;

Correspondence to: Weihong Tan.

Fax: (+1)352-846-241 tan@chem.ufl.edu.

**Supporting Information Available:** Schematic represent of the sequence of DNA for constructing walking system, native gel electrophoresis to demonstrate walking system construction, FRET between Dabcyl/FAM and between Dabcyl/TAMRA, processive motion of the walker along the track, and fluorescence measurement and calibration curve for right/left turning choice. This material is available free of charge *via* the Internet at <http://pubs.acs.org>.

they are not as powerful or organized as their natural protein counterparts. In this regard, identification of new types of energy supplies could be meaningful in the development of the next-generation mechanical robots, ideally with more powerful and controllable operation.<sup>3</sup>

We recently reported a new light energy-powered DNA walker, which is capable of regulated autonomous movement along a nucleic acid track.<sup>17</sup> Construction of free-running and autonomous motors, which remain in operation as long as a source of energy is available, is essential to the operation of nanomachines that mimic biological function. However, the capability of autonomous motion sometimes results in decreased controllability. That is, the device cannot be easily stopped at a desired position or time, or once stopped, it is difficult to restart. The availability of an easily-controllable, free-running walking device would also be significant for the future design of nanorobots to perform multiple and complex functions. We have demonstrated that photochemical energy sources can serve as inputs in the operation of nanosized DNA walkers, where light-initiated chemical cleavage allows precise control of the speed and motion of autonomous nanorobots.<sup>17,18</sup>

The directional movement of the above-mentioned light-driven walker stems from the “burnt-bridge” mechanism, whereby the anchorage sites on the track are irreversibly consumed during the motion. However, as a result, the reversible, cyclic operation of the walking device has been eliminated, preventing the walker from mimicking natural molecular motors (*e.g.*, kinesin) that change the directionality of movement towards both ends of the tracks,<sup>2</sup> and seriously restricting future usage of the device for multiple trips. Advancing the functions of the walking system to facilitate reversible and multi-directional locomotion is one goal of DNA engineering. In the present work, we describe a new light-driven walking system, which enables the DNA walker to travel in either direction on the track, with precise controllability, by using different wavelengths of light irradiation.

## RESULTS AND DISCUSSION

The movement of the DNA walker is guided by the prescriptive landscape. Through precise specification of walker/ environment interactions, directional locomotion can be realized without a cleavage process. In DNA strand exchange, one prehybridized strand in a DNA duplex is displaced by an invading strand. The rate of strand exchange can be quantitatively controlled by varying the length of toeholds (short single-stranded domains to initiate displacement).<sup>19,20</sup> Based on toehold-mediated strand displacement, we demonstrate in this study the reversible, autonomous and controllable movement of DNA walkers along an azobenzene-incorporated prescriptive track.

The walking system consists of three parts: a single-stranded DNA track (**T**), several photosensitive anchorage sites (*e.g.*, **S1** and **S2**), and a DNA walker (**W**) (Figure 1). The track contains three 21-nucleotide (nt) long binding regions that are complementary to the recognition tags of the respective anchorage sites. Through specific DNA interaction, the track organizes the anchorage sites into one self-assembled construction, with the walker (**W**) binding sites extending from the track. After assembly, the distance between two adjacent anchorage sites corresponds to two helical pitches, roughly 7nm. The construction of the overall walking system was verified by native polyacrylamide gel electrophoresis (Figure S1 in the Supporting Information).

The DNA walker contains two legs, a searching leg and a holding leg, and they are linked by a DNA oligomer as the body. The two motion legs are designed to respectively bind the two extender segments of each anchorage site. The holding leg binds the 16-nt extender segment,

which is identical in all anchorage sites to prevent the walker from leaving the track. The other extender segment, which serves as the toehold to mediate the locomotion (strand displacement) of the walker, is designed to be complementary with the searching leg of the DNA walker.

Various numbers of azobenzene moieties were incorporated into different extender segments. The photoinduced isomerization of azobenzene molecules has been broadly used to induce significant conformational and biochemical changes in nucleic acids,<sup>21-25</sup> peptides and proteins.<sup>26</sup> The light-driven *cis/trans* isomerization of the azobenzene moiety is wavelength-dependent: UV light at 365nm drives the *trans*-to-*cis* conversion, while visible light at around 465nm corresponds to the *cis*-to-*trans* isomerization. When incorporated into the DNA structure, the UV light-induced *cis*-form lowers the binding affinity of the DNA duplex based on the spatial hindrance to DNA hybridization. In contrast, visible light irradiation reverses the isomerization and enables DNA duplex binding. By introducing azobenzene moieties into the toehold domain of extender segments, the moving direction of the walker (*i.e.*, the strand-displacement pathway towards the longer toehold binding site) is controllable by irradiation with different wavelengths of light (Figure 1).

The directional locomotion of the DNA walker was investigated using a fluorescence resonance energy transfer (FRET) assay. As the FRET acceptor, Dabcyl quencher was labeled on the walker's holding leg, and fluorescence donors, 6-carboxyfluorescein (6-FAM) and tetramethylrhodamine (TAMRA), were attached to anchorage sites **S1** and **S2**, respectively (Figure S2 in the Supporting Information). Because FRET efficiency is proportional to the inverse 6<sup>th</sup> power of the donor-acceptor distance, FRET is expected to occur most efficiently when the walker steps onto the respective anchorage site, thereby bringing FAM (or TAMRA) and Dabcyl together.

We first tested the feasibility of our method by using the simplest two-step photocontrollable locomotion (Figure 2a). The FAM-labeled **S1** anchorage site containing 7 nucleotides (7-nt) served as the toehold domain for binding the searching leg of the DNA walker. In comparison, the TAMRA-labeled **S2** site containing a longer toehold region (14-nt) also included nine azobenzene moieties (one after every two bases, see Experimental Section). Such azobenzene/nucleic acid ratio has previously been proven to be highly efficient in regulating DNA hybridization efficiency.<sup>21-25</sup> Based on the “nearest-neighbor model” of azobenzene-incorporated DNA duplex formation,<sup>25</sup> a full thermodynamic description has been presented and successfully used to predict the melting temperature of azobenzene-incorporated DNA duplexes. Under visible light, the *trans*-form of azobenzene facilitates DNA duplex binding, and the longer toehold within the **S2** anchorage mediates the directional motion of walker from **S1** to **S2** site. In contrast, UV light irradiation induces the *trans*-to-*cis* isomerization of azobenzene and reduces the length of the available toehold within the **S2** anchorage site to reverse the direction of motion (**S2** to **S1**).

Using locomotion from **S2** to **S1** as an example, the assumption was experimentally tested. The walker was specifically positioned on the **S2** site through separately prepared **T**(track)-**S1** and **S2-W**(walker) conjugates (Figure S1 in the Supporting Information). Mixing the conjugates immediately prior to light irradiation ensured that the **S2** anchorage would be the initiating site (the largest distribution binding position) for the walker. Indeed, consistent with our expectation, directional walking pathways, *i.e.*, **S1**→**S2** under visible light (azobenzene *trans*) and **S2**→**S1** under UV light (azobenzene *cis*), were observed (Figure 2). When initiated at the **S2** site, **W** was expected to stay under the visible light, instead of stepping onto the **S1** site. Following the expected motional mode, irradiation for the first 1000s with visible light (450nm, Figure 2b) did not have a great effect on the fluorescence

from either FAM or TAMRA; however, UV light irradiation (365nm) immediately initiated the quenching of the FAM signal and the recovery of TAMRA fluorescence.

As control, it was demonstrated that the same UV light does not affect the fluorescence signal of either dye (data not shown); the fluorescence change was indeed associated with locomotion of the walker from **S2** to **S1** site. In another control experiment, we demonstrated that the free anchorage site (with the same legs as **S2**) under the same conditions would not disturb migration of the walker between **S1** and **S2** along the track (Figure S3 in the Supporting Information). This observation is important in proving that the DNA walker remains attached to the same track during the entire operation. Such “processive” locomotion<sup>3</sup> prevents formation of a “bridge” between two tracks and forces the walker to move a longer distance along the track.

The reversible movement of the walker along this photocontrollable track was also verified. As shown in Figure 2c, by alternating the wavelength of light (450nm or 365nm), the direction of locomotion was switched accordingly. At the end of each cycle of light irradiation, the device can be reset, and the walker is able to repeatedly perform similar mechanical motion. It is noteworthy that such reversible locomotion cannot be achieved by movements based on the above-mentioned “burnt-bridge” mechanism whereby the track is irreversibly damaged during passage. Furthermore, no waste molecules (neither DNA duplex<sup>27,28</sup> nor chemical triggers<sup>29,30</sup>) accumulate during the reversible operation, an important consideration for the continuous long-term usage of the walking device.

When given a selection of routes in multipath systems, DNA walkers based on the “burnt bridge” mechanism will lose control of direction, with equal chance of moving on either path. This difficulty is viewed as one of main challenges for active DNA nanostructures.<sup>10,31,32</sup> However, we have demonstrated that route selection can be easily achieved in this azobenzene-modified walking device *via* irradiation with different wavelengths of light. As shown in Figure 3, a **S0** anchorage site was introduced between the above-mentioned **S1** and **S2** sites, as the initiating binding site (crossing point) for the walker. When irradiated with visible light, after 50 minutes incubation, *c.a.* 94% of the walker strands move to the **S2** site (longer toehold and faster, more stable binding), and only 6% of the strands bind to **S1**. In another study, under UV light, as expected, more walker strands turned to the **S1** site (69% at equilibrium) compared with **S2** (31%, see Figure S4 in the Supporting Information). With UV light irradiation, it was also proven that 1) it takes longer for walkers to choose the route and 2) the final walker strand distribution is less controllable. This result is associated with the fact that a smaller toehold length difference (comparing that between **S1** and **S0** sites with that of between **S2** and **S0**) can result in a longer time to reach equilibrium and a smaller equilibrium constant.<sup>19,20</sup> Potentially, this process could be further optimized by varying the numbers of toehold nucleotides and azobenzenes in the anchorage sites.

Finally, we wanted to prove that movement over a longer distance can be achieved by logical programming of the anchorage sites. As an example, an **S2\*** anchorage site was introduced between **S1** and **S3** sites (with the same extender segments as **S2**, Experimental Section), with the distance from each site as 7nm (Figure 4a). With visible irradiation, **S2\*** has a 10-nt-long segment in between **S1** (7-nt) and **S3** (14-nt) to bind with the walker's searching leg. The toehold length difference mediates the movement in the direction of **S1**→**S2\***→**S3**. Moreover, these three anchorage sites were designed with various numbers of azobenzene moieties: 0, 3 and 9 for **S1**, **S2\*** and **S3**, respectively. These numbers were selected so that the binding strength with the DNA walker followed the order of **S1**>**S2\***>**S3** under UV light,<sup>25</sup> because *trans*-to-*cis* isomerization of the azobenzene moieties results in a different degree of change to the three sites. Based on the switched toehold length and

dynamic binding affinity, the walker should preferentially move in the direction of  $S3 \rightarrow S2^* \rightarrow S1$ , reversing the previous movement.

As demonstrated from the fluorescence measurements (Figure 4), when walking was initiated at **S1** site (visible light irradiation), about an hour on average was required to pass through TAMRA-modified **S2\*** (minimum fluorescence) and further move on to the **S3** site (recovered TAMRA fluorescence). Under UV light irradiation, the reverse motion was demonstrated, starting from **S3** site, passing through **S2\*** (minimum TAMRA fluorescence), and finally reaching the **S1** destination (recovered TAMRA fluorescence), proving that the walker can move in either direction along a prescriptive photo-switchable track.

## CONCLUSIONS

Based on the isomerization of azobenzene moieties and toehold-mediated strand displacement, we have designed a light-controlled DNA walking device that can move to either end of the oligonucleotide track, and the direction of motion can be switched using different wavelengths of light. Compared with other reported DNA walkers,<sup>3-17</sup> this new strategy not only preserves the autonomous and controllable movement, but also provides a reusable track, making it feasible to reset the device after the complete trip, as observed in nature for kinesin and myosin.<sup>1,2</sup> So far, the rate and step number of this device are still limited, which might be due to the imperfect photoisomerization efficiency of the azobenzene moieties. However, the principle of photoisomerization-induced toehold length switching could be further used in designing other autonomous DNA-based walking devices, where sequential and controllable release of the toehold is required.<sup>8-11</sup> Moreover, as the first study (based on our knowledge) of using photoswitchable molecules for alternating the DNA toehold binding regions, this system can be employed for external control of the route selection in multi-pathway systems, *e.g.*, “crossing” or “T junction”, for more advanced walking devices that can rival molecular motors in nature.

## MATERIALS AND METHODS

### Oligonucleotides

All oligonucleotides were synthesized using an ABI 3400 DNA synthesizer (Applied Biosystems, Inc., Foster City, CA). The DNA sequences employed in this study: Track **T<sub>1-2\*3</sub>**: 5'-ACC ATC TGT GGC ATA GCA GCG AGT ATC TAA CGC ATG GAA GCG TCG ATC TTG AGC ATT GGA GCG-3'; **T<sub>1-0-2</sub>**: 5'-AGT ATC TAA CGC ATG GAA GCG ACC ATC TGT GGC ATA GCA GCG TCG ATC TTG AGC ATT GGA GCG-3'; **T<sub>1-2</sub>**: 5'-AGT ATC TAA CGC ATG GAA TCG ATC TTG AGC ATT GGA GCG-3'; Anchorage site **S0**: 5'-GTC CGA ATC AGC ACT TTC GCT GCT ATG CCA CAG ATG GT-3'; **S1**: 5'-GTC ACT CTTGTC CGA ATC AGC ACT -FAM-TTC GCT CCA ATG CTC AAG ATC GA-3'; **S2**: 5'-CA Z-TT-Z-GG-Z-AG-Z-TC-Z-AC-Z-TC-Z-TT-Z-GT-Z-C CGA ATC AGC ACT -TAMRA-TTC GCT TCC ATG CGT TAG ATA CT-3'; **S2\***: 5'-GGZ-AG-Z-TC-Z-ACT CTTGTC CGA ATC AGC ACT -TAMRA-TTC GCT TCC ATG CGT TAG ATA CT-3'; **S3**: 5'-CA-Z-TT-Z-GG-Z-AG-Z-TC-Z-AC-Z-TC-Z-TT-Z-GT-Z-C CGA ATC AGC ACT TTC GCT GCT ATG CCA CAG ATG GT-3'; Walker **W**: 5'-Dabcyl-AGT GCT GAT TCG GAC AGG CTA GCT ACA ACG AGA GTG ACT CCA ATG-3' (**T<sub>1-2</sub>** = track to arrange anchorage site in the order of **S1-S2**; Z = azobenzene-modified position in the anchorage site).

### Manipulation of the Walking System

Using  $S3 \rightarrow S2^* \rightarrow S1$  as an example, the formation of the walking system was as follows. After separate annealing (95°C-10°C, over 20 min) in 25mM Tris buffer (pH=7.5,

containing 50mM NaCl and 5mM MgCl<sub>2</sub>), **T-S1-S2\*** and **S3-W** conjugates were mixed to give a final concentration for each sequence of 0.1μM, and the sample was irradiated with either a 6W portable UV lamp (60 Hz with center wavelength at 365 nm and measured light source power around 0.2mW) or a table lamp (60Hz, 120V with 60W bulb and measured light source power 30mW). The irradiation power employed was measured using a power meter (Newport Corp., Irvine, CA). During irradiation, the temperature of the sample was maintained at 23.0°C using a water bath (ThermoNESLAB Inc.). After a series of irradiation times, the samples were removed and subjected to FRET experiments.

### FRET Measurements

A FluoroMax-4 Spectrofluorometer with a temperature controller (Jobin Yvon) was used for all steady-state fluorescence measurements. After a series of irradiation time periods, fluorescence intensities at 515nm (FAM,  $\lambda_{ex}$ =488nm; slit number=5nm, 0.2s integration time) and 580nm (TAMRA,  $\lambda_{ex}$ =550nm; slit number=5nm, 0.2s integration time) were recorded, with temperature controlled at 23°C.

### Native PAGE Analysis

The binding and three-dimensional structures of the DNA walking system were observed using native PAGE gel. Normally the gel was run in 8-10% acrylamide (containing 19/1 acrylamide/bisacrylamide) solution with 1×TBE/15mM Mg<sup>2+</sup> buffer, at 100V constant voltage for 1 hour (4°C). After that, the gel was stained 30 min using Stains-All (Sigma-Aldrich) to image the position of DNA. Photographic images were obtained under visible light with a digital camera.

### Supplementary Material

Refer to Web version on PubMed Central for supplementary material.

### Acknowledgments

We acknowledge Dr. K. R. Williams for manuscript review. This work is supported by grants awarded by the National Institutes of Health (GM066137, GM079359 and CA133086) and by NSF. M.Y. would like to thank the Eastman Co. Fellowship (Kingsport, TN) for support.

### REFERENCES

1. Schliwa M, Woehlke G. Molecular Motors. *Nature*. 2003; 422:759–765. [PubMed: 12700770]
2. Roostalu J, Hentrich C, Bieling P, Telley I-A, Schiebel E, Surrey T. Directional Switching of the Kinesin Cin8 Through Motor Coupling. *Science*. 2011; 332:94–99. [PubMed: 21350123]
3. Von Delius M, Leigh D-A. Walking Molecules. *Chem. Soc. Rev.* 2011; 40:3656–3676. [PubMed: 21416072]
4. Bath J, Turberfield A-J. DNA Nanomachines. *Nat. Nanotechnol.* 2007; 2:275–284. [PubMed: 18654284]
5. Barrell M-J, Compana A-G, von Delius M, Geertsema E-M, Leigh D-A. Light-Driven Transport of a Molecular Walker in Either Direction Along a Molecular Track. *Angew. Chem., Int. Ed.* 2011; 50:285–290.
6. Gu H, Chao J, Xiao S, Seeman N-C. A Proximity-based Programmable DNA Nanoscale Assembly Line. *Nature*. 2010; 465:202–205. [PubMed: 20463734]
7. He Y, Liu D-R. Autonomous Multistep Organic Synthesis in a Single Isothermal Solution Mediated by a DNA Walker. *Nat. Nanotechnol.* 2010; 5:778–782. [PubMed: 20935654]
8. Yin P, Choi H-M-T, Calvert C-R, Pierce N-A. Programming Biomolecular Self-Assembly Pathways. *Nature*. 2008; 451:318–322. [PubMed: 18202654]



9. Omabegho T, Sha R, Seeman N-C. A Bipedal DNA Brownian Motor with Coordinated Legs. *Science*. 2009; 324:67–71. [PubMed: 19342582]
10. Muscat R-A, Bath J, Turberfield A-J. A Programmable Molecular Robot. *Nano Lett.* 2011; 11:982–987. [PubMed: 21275404]
11. Green S-J, Bath J, Turberfield A-J. Coordinated Chemomechanical Cycles: a Mechanism for Autonomous Molecular Motion. *Phys. Rev. Lett.* 2008; 101:238101. [PubMed: 19113596]
12. Lund K, Manzo A-J, Dabby N, Michelotti N, Johnson-Buck A, Nangreave J, Taylor S, Pei R, Stojanovic MN, Walter N-G, et al. Molecular Robots Guided by Prescriptive Landscapes. *Nature*. 2010; 465:206–210. [PubMed: 20463735]
13. Tian Y, He Y, Chen Y, Yin P, Mao C. A DNAzyme that Walks Processively and Autonomously Along a One-Dimensional Track. *Angew. Chem., Int. Ed.* 2005; 44:4355–4358.
14. Bath J, Green S-J, Tuberfield A-J. A Free-Running DNA Motor Powered by a Nicking Enzyme. *Angew. Chem., Int. Ed.* 2005; 44:4358–4361.
15. Wickham S-F-J, Endo M, Katsuda Y, Hidaka K, Bath J, Sugiyama H, Turberfield A-J. Direct Observation of Stepwise Movement of a Synthetic Molecular Transporter. *Nat. Nanotechnol.* 2011; 6:166–169. [PubMed: 21297627]
16. Yin P, Yan H, Daniell X-G, Turberfield A-J, Reif J-H. A Unidirectional DNA Walker that Moves Autonomously Along a DNA Track. *Angew. Chem., Int. Ed.* 2004; 43:4906–4911.
17. You M, Chen Y, Zhang X, Liu H, Wang K, Wang R, Williams KW, Tan W. An Autonomous and Controllable Light-Driven DNA Walking Device. *Angew. Chem., Int. Ed.* 2012; 51:2457–2460.
18. You M, Zhu Z, Liu H, Gulbakan B, Han D, Wang R, Williams KR, Tan W. Pyrene-Assisted Efficient Photolysis of Disulfide Bonds in DNA-based Molecular Engineering. *ACS Appl. Mater. Interfaces*. 2010; 2:3601–3605. [PubMed: 21080636]
19. Zhang D-Y, Seelig G. Dynamic DNA Nanotechnology Using Strand-Displacement Reactions. *Nat. Chem.* 2011; 3:103–113. [PubMed: 21258382]
20. Genot A-J, Zhang D-Y, Bath J, Turberfield A-J. Remote Toehold: a Mechanism for Flexible Control of DNA Hybridization Kinetics. *J. Am. Chem. Soc.* 2011; 133:2177–2182. [PubMed: 21268641]
21. Liang X, Mochizuki T, Asanuma H. A Supra-Photo Switch Involving Sandwiched DNA Base Pairs and Azobenzenes for Light-Driven Nanostructures and Nanodevices. *Small*. 2009; 5:1761–1768. [PubMed: 19572326]
22. Zhou M, Liang X, Mochizuki T, Asanuma H. A Light-Driven DNA Nanomachine for Efficiently Photoswitching RNA Digestion. *Angew. Chem., Int. Ed.* 2010; 49:2167–2170.
23. Kang H, Liu H, Phillips J-A, Cao Z, Kim Y, Chen Y, Yang Z, Li J, Tan W. Single-DNA Molecular Nanomotor Regulated by Photons. *Nano Lett.* 2009; 9:2690–2696. [PubMed: 19499899]
24. You M, Wang R, Zhang X, Chen Y, Wang K, Peng L, Tan W. Photo-Regulated DNA-Enzymatic Nanostructures by Molecular Assembly. *ACS Nano*. 2011; 5:10090–10095. [PubMed: 22098552]
25. Asanuma H, Matsunaga D, Komiyama M. Clear-Cut Photo-Regulation of the Formation and Dissociation of the DNA Duplex by Modified Oligonucleotide Involving Multiple Azobenzenes. *Nucleic. Acids. Symp. Ser.* 2005; 49:35–36.
26. Schierling B, Noel A-J, Wende W, Hien Le T, Volkov E, Kubareva E, Oretskaya T, Kokkinidis M, Rompp A, Spengler B, et al. Controlling the Enzymatic Activity of a Restriction Enzyme by Light. *Proc. Natl. Acad. Sci. USA*. 2010; 107:1361–1366. [PubMed: 20080559]
27. Shin J, Pierce N-A. A Synthetic DNA Walker for Molecular Transport. *J. Am. Chem. Soc.* 2004; 126:10834–10835. [PubMed: 15339155]
28. Sherman W-B, Seeman N-C. A Precisely Controlled DNA Biped Walking Device. *Nano Lett.* 2004; 4:1203–1207.
29. Wang Z, Elbaz J, Willner I. DNA Machines: Bipedal Walker and Stepper. *Nano Lett.* 2011; 11:304–309. [PubMed: 21166467]
30. Wang C, Ren J, Qu X. A Stimuli Responsive DNA Walking Device. *Chem. Comm.* 2011; 47:1428–1430. [PubMed: 21152587]
31. Pinheiro A-V, Han D, Shih W-M, Yan H. Challenges and Opportunities for Structural DNA Nanotechnology. *Nat. Nanotechnol.* 2011; 6:763–772. [PubMed: 22056726]

32. Wickham S-F-J, Bath J, Katsuda Y, Endo M, Hidaka K, Sugiyama H, Turberfield A-J. A DNA-based Molecular Motor that Can Navigate a Network of Tracks. *Nat. Nanotechnol.* 2012; 7:169–173. [PubMed: 22266636]



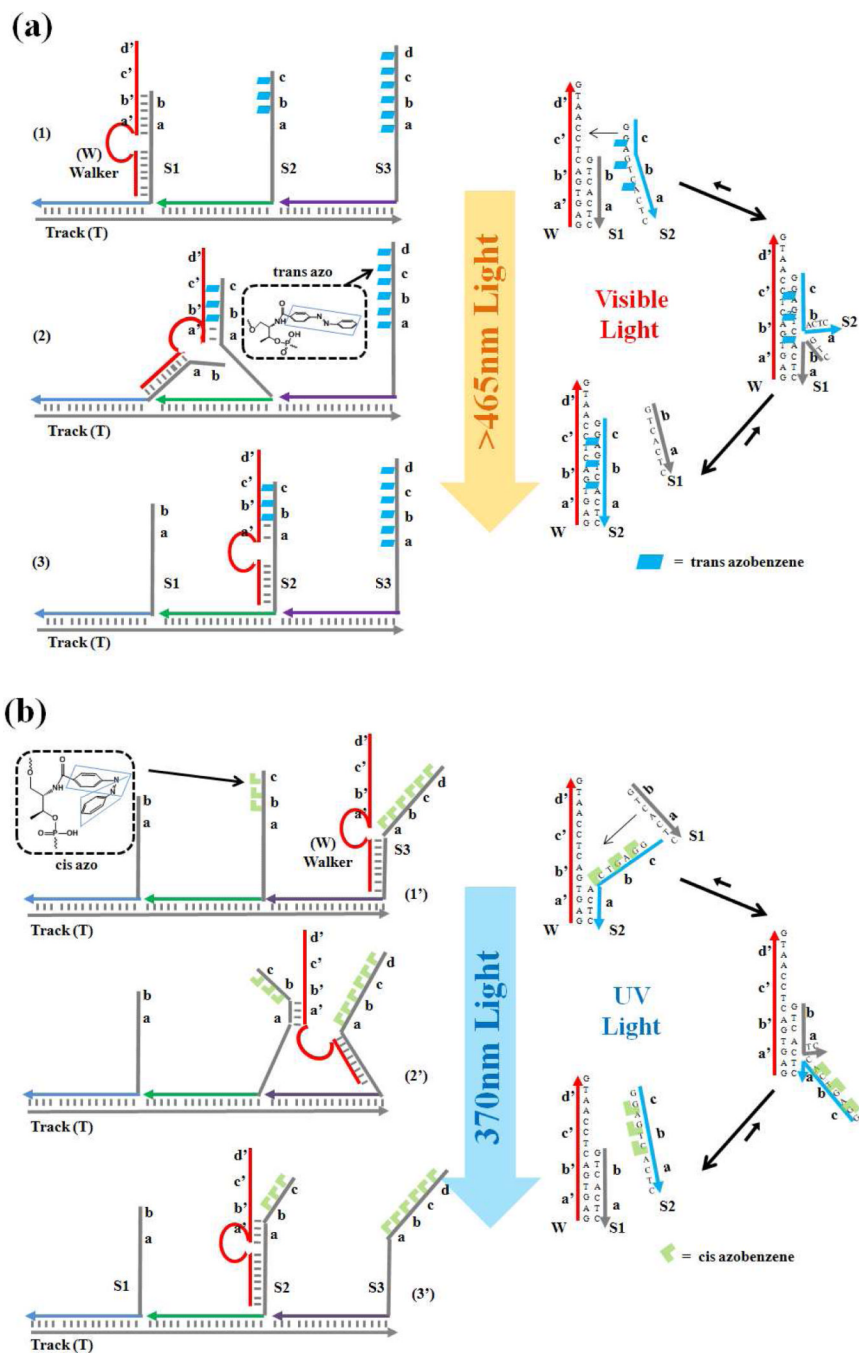


**Figure 1.** Principle of the DNA-based walking device. Walker, anchorage sites, and track form the walking system through self-assembly; the locomotion of the walker is realized through toehold-mediated strand displacement. (a) Visible light irradiation (azobenzene, *trans*) triggers walker motion in the direction of S1→S3; (b) UV light (azobenzene, *cis*) induces the reverse movement of S3→S1. (Domains a, b, c and d are complementary to a', b', c' and d', respectively).

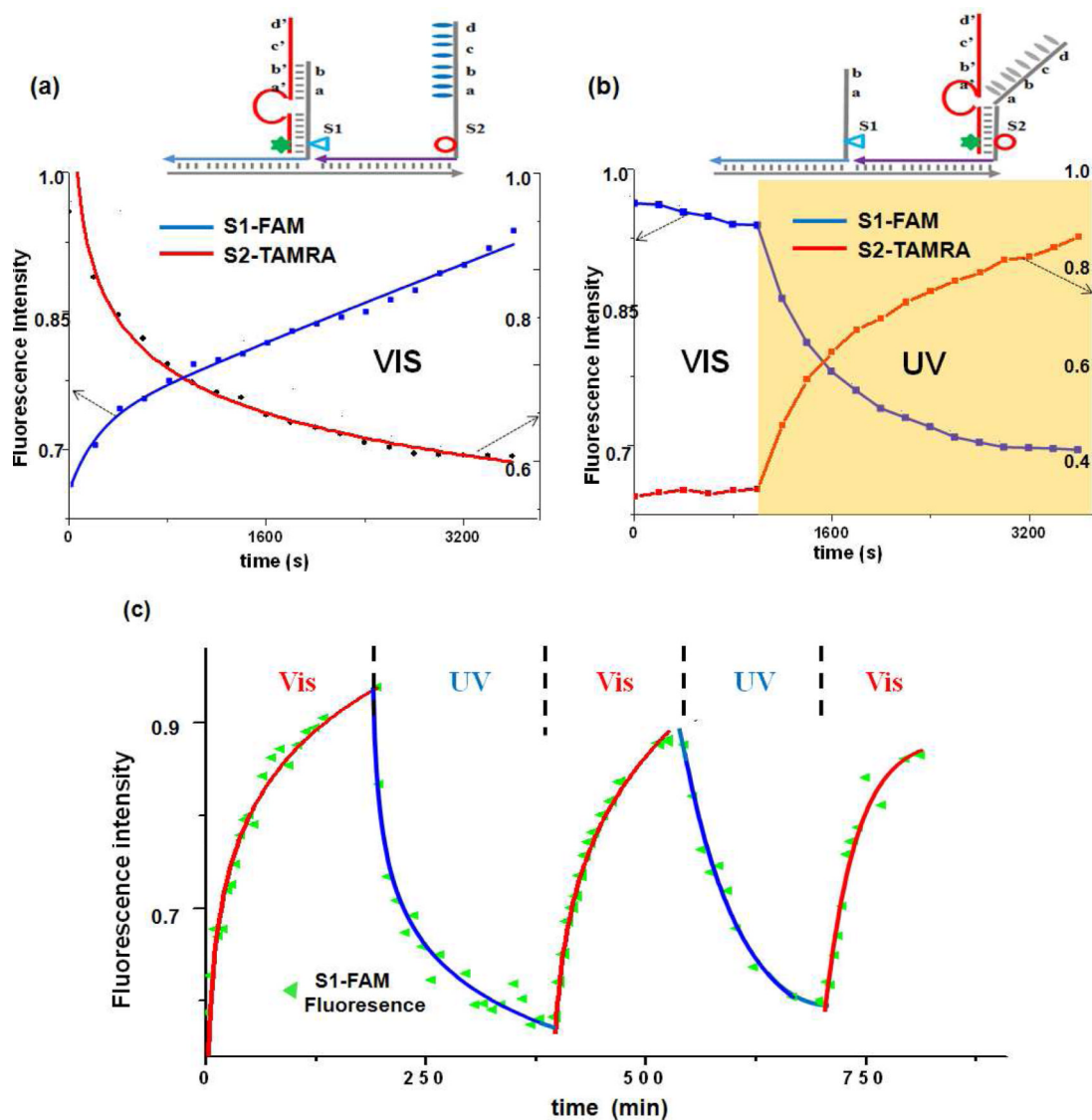


**Figure 2.** Progressive and reversible walking demonstrated by FRET assay. Dabcyl (quencher, star)-labeled walker moves on the anchorage site labeled with fluorophore TAMRA (circle) and FAM (triangle). Fluorescence intensity (515nm for FAM,  $\lambda_{ex}=488\text{nm}$ ; 580nm for TAMRA,  $\lambda_{ex}=550\text{nm}$ ) was monitored during (a) **S1**→**S2** locomotion (continuous visible irradiation), (b) **S2**→**S1** locomotion (visible irradiation for 1000s followed by UV irradiation), and (c) the reversible movement of the walker during the alternate period of UV and visible irradiation.

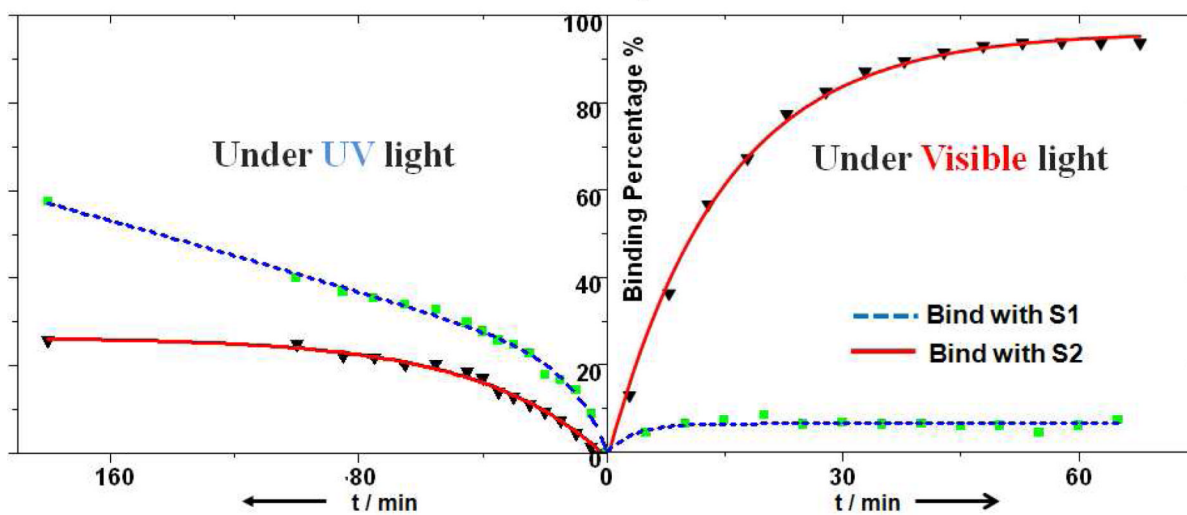
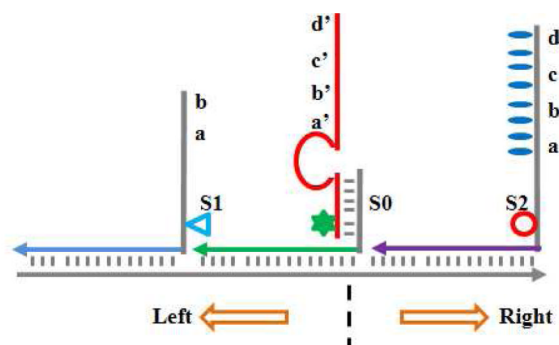


**Figure 3.**

Programmed control of route selection at a junction. Left turn ( $S0 \rightarrow S1$ ) was achieved under UV light irradiation, and right turn ( $S0 \rightarrow S2$ ) was induced by visible light. The fractions of the walker (labeled with Dabcyl, star) moving towards  $S2$  (labeled with TAMRA, circle) or  $S1$  (labeled with FAM, triangle) were monitored based on the fluorescence intensity change and further calculated using a standard calibration curve.

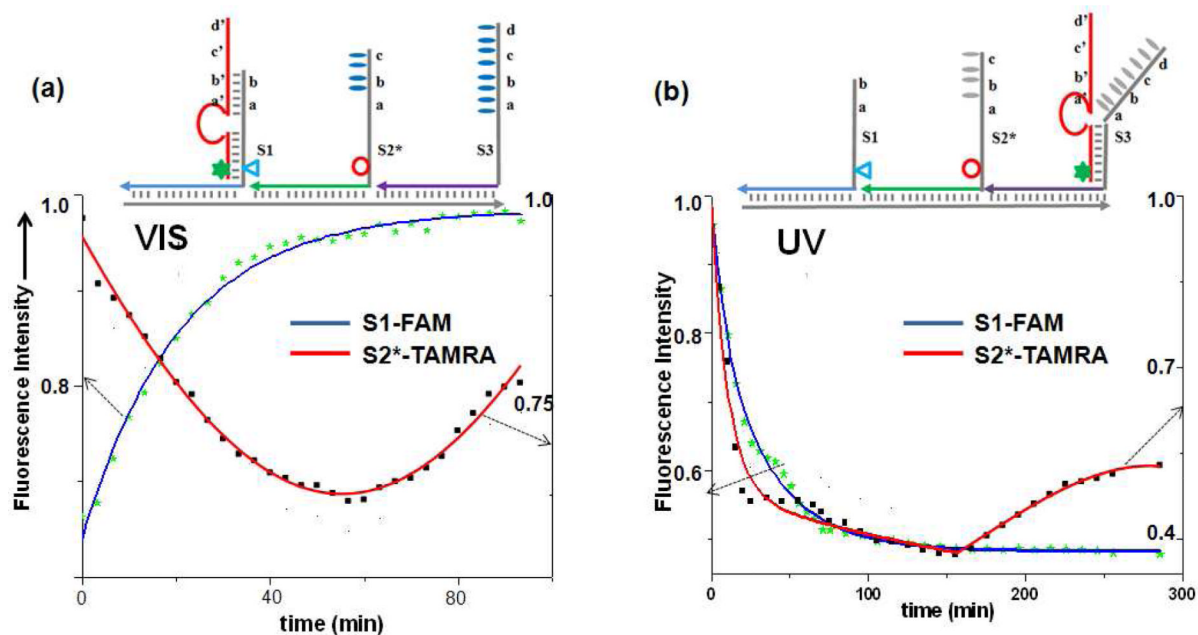


**Figure 4.**

Progressive operation of the walker on a 3-step track. Motion was demonstrated in the direction of  $S1 \rightarrow S2^* \rightarrow S3$  under visible light, and it was reversed to follow the  $S3 \rightarrow S2^* \rightarrow S1$  direction with UV irradiation. Fluorescence intensity was monitored at 515nm for FAM (triangle)-labeled  $S1$  site ( $\lambda_{ex} = 488\text{nm}$ ) and at 580nm for TAMRA (circle)-labeled  $S1^*$  site ( $\lambda_{ex} = 550\text{nm}$ ).